Fachtagung "Lasermethoden in der Strömungsmesstechnik"
8. – 10. September 2015, Dresden

Bestimmung der tangentialen Geschwindigkeiten in freien Oberflächenwirbeln mittels Highspeed PIV-Messungen

Determination of tangential velocities in free surface vortices by high-speed PIV measurements

Nicolai Szeliga, Steffen Richter, Daniel Bezecny, Michael Schlüter
Institute of Multiphase Flows, Hamburg University of Technology, Eißendorfer Str. 38, 21073 Hamburg, Germany

Highspeed PIV; Tangentialgeschwindigkeit; freie Oberflächenwirbel; Hochleistungs-LED
High-speed PIV; tangential velocity; free surface vortex; High Power-LED

Abstract

High-speed Particle Image Velocimetry (PIV) measurements were realized in a laboratory scale setup, to investigate the tangential velocity profile of free surface air core vortices thereby obtaining the necessary data to validate a modified Burgers-Rott model.
The experiments were conducted in a transparent, cylindrical vessel with a constant submergence and cylindrical outlet geometry to investigate the fluid dynamics leading to air core vortices. Inlet geometries with a circular cross section created an inflow with a defined angular momentum to obtain a symmetrical velocity field. Image recording was performed, using a High Power-LED System together with a high-speed CCD camera. The camera was mounted below the vessel, directly next to the outlet. This setup enables detailed measurements of the tangential velocity field inside the vortices from a horizontal plane at different heights and varying Froude numbers, while avoiding both surface reflections by laser light illumination and flow disturbances.

Introduction

The occurrence of vortices in cooling water reservoirs poses a high safety risk for the safe operation of cooling systems. Vortices lead to entrainment of angular momentum and gas in cooling pumps which reduces or interrupts the flow of cooling water and damages pump inlets, see Knauss 1983. The prevention of air entraining vortices has therefore a high priority, when designing a cooling system. Air entrainment occurs, when the water level drops below the critical submergence of the outlet, see Hecker 1987.
Since the occurrence of vortices depends on various independent parameters, like the reservoir and outlet geometries, volume flow rates, angular momentum and submergence, methods to calculate the critical submergence are either rough approximations or theoretical models with limited practical value, see Pandazis et al. 2010. The analytical vortex model by Burgers & Rott, even though introduced first in 1958, proves to be a very accurate model to describe symmetrical vortices. The Burgers-Rott model is based on the 2D-Navier-Stokes equations with the assumptions of a steady, axisymmetric and incompressible flow. With these assumptions the velocities in tangential, radial and axial direction can be calculated with

$$u_t = -\frac{\Gamma_\infty}{2r\pi}\left[1-\exp\left\{-\left(\frac{r}{r_0}\right)^2\right\}\right], \text{with } r_0 = 2\sqrt{\frac{\nu}{a}} \quad (1)$$

$$u_r = -\frac{1}{2}ar \tag{2}$$

$$u_z = a(h - h_\infty). \tag{3}$$

Here Γ_∞ is the circulation and h_∞ the submergence outside of the vortex core, r is the radius, ν is the kinematic viscosity and a is the suction parameter, a variable based on the intensity of the axial velocity gradient, see Rott 1958 and Burgers 1948.
Ito et al. have made a modification on the Burgers & Rott model which leads to a simple equation for the air core length L

$$L = \lim_{r\to\infty} h(r) - h(0) \approx \frac{a\cdot\ln(2)}{\nu\cdot g}\left(\frac{\Gamma_\infty}{4\pi}\right)^2, \tag{4}$$

which only needs two parameters to calculate the vortex strength, the Circulation Γ_∞ and the suction parameter a, see Ito et al. 2010.
An earlier attempt to calculate the tangential velocity and the air core length of a free surface vortex is the vortex model of Rankine first introduced in 1858. The Rankine vortex model uses a combined method to calculate the tangential velocity profile of a free surface vortex. The same assumptions as in the model of Burgers & Rott are used, but additionally the vortex core is viewed as a solid-body rotation. Therefore the tangential velocity profile is calculated as

$$u_t = \frac{\Gamma_\infty}{2\pi}\frac{r}{r_m^2}, \quad r \le r_m \tag{5}$$

and

$$u_t = \frac{\Gamma_\infty}{2\pi r}, \quad r > r_m \tag{6}$$

with r_m as the radius of the vortex core, see Batterson et al. 2007. Both, the Burgers-Rott, as well as the Rankine model, result in the same tangential velocity maximum at the border of the vortex core, as can be seen in Fig. 1. Modifications to the Rankine vortex model have been made among others by Odgaard 1986 and Chen et al. 2007.

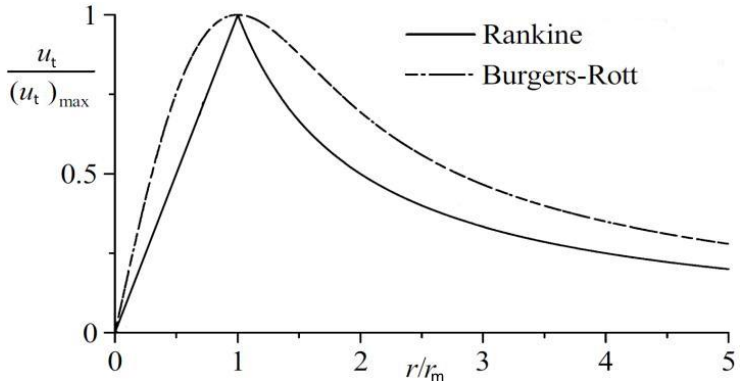

Figure 1: Comparison of the dimensionless tangential velocity profiles of the Rankine and the Burgers & Rott vortex models over the dimensionless radius see Batterson et al. 2007.

To allow a comparison with future measurements (in upscaled experiments) the volume flow will be converted to Froude numbers Fr with

$$Fr = \frac{u}{\sqrt{g \cdot d}} \tag{7}$$

where u is the velocity in the outlet, and d is the diameter of the outlet.
There have been recent publications regarding PIV and also Particle Tracking Velocimetry (PTV) measurements of air entraining vortices, most notably by Keller et al. 2014 for PIV and Suerich-Gulick et al. 2014 for PTV measurements. Suerlich-Gulick et al. investigate a vertical outlet pipe while Keller et al. investigate a horizontal outlet pipe. Both research groups use setups with a uniform inflow from one side of a rectangular basin, which don't factor the induction of angular momentum. With the experimental setup introduced in this paper it is possible to measure the effect of an induced angular momentum on an air core vortex and its tangential velocity profile.

Methods

The investigations of the tangential velocity fields are conducted in a laboratory scale vessel filled with deionized water, see Fig. 2 for a flowsheet of the experimental setup. The vessel is build from transparent Poly(methyl methacrylate) (PMMA) and has a cylindrical shape with an inner diameter of d_V = 0.288 m. The outlet is centered in the middle of the bottom of the vessel with a cylindrical shape and a diameter of d_{out} = 15 mm. Behind the outlet a 90° pipe bend redirects the flow in horizontal direction towards a circular pump. From the pump the flow runs through a tubular heat exchanger. After the heat exchanger the flow is divided by a bypass which directs one part of the flow back to the suction side of the pump. The remaining flow runs through a volumetric flow meter (Endress+Hauser Promass 80F) and is separated into four flows which are leading to the inlets of the vessel. The inlets consist of steel tubes with an inner diameter of d_{in} = 16 mm, bend in a 45° angle towards the vertical axis. The four inlet pipes with a circular cross section, shown in Fig. 3a, induce a stable flow with a defined angular momentum.

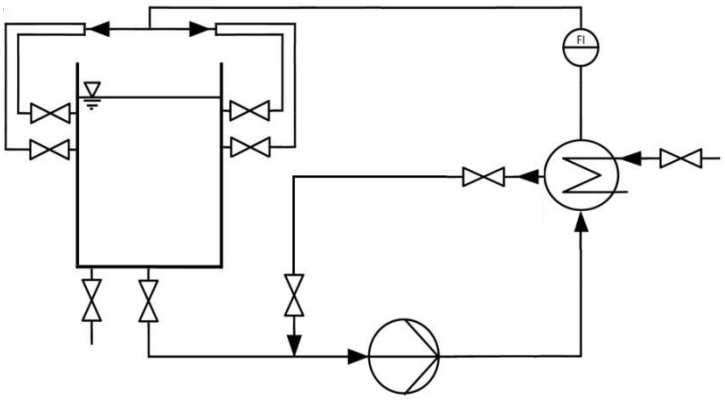

Figure 2: flowsheet of the experimental setup.

The measurement of the horizontal velocity fields is conducted with a High-speed CCD-Camera/High Power-LED system. The high-speed CCD-Camera (PCO Dimax H2) is implemented directly below the bottom of the vessel as close as possible to the outlet. The lens is adjusted to the minimal f-number of 2 to gain a thin depth of focus. The High Power-LED (LPS - LED Pulsing System, ILA GmbH) is implemented orthogonally to the camera and the vertical axis of the vessel, see Fig. 3b for a drawing of the setup. The LED emits light in the visible blue spectrum with a wave length distribution of λ = 454 - 462 nm and a maximum at λ = 460 nm. A collimator lens focuses the emitted light into a homogenous beam with a diameter of 30 mm. Camera and LED System are connected via a synchronizer and both operate

with a sample rate of 1000 Hz, while pulse length and exposure time are set to 10 µs. The emitted energy output of the LED is around 0.9 mJ per pulse. The CCD sensor of the camera has a spatial resolution of 1.5 Mpx (1400 x 1050 px) and an intensity resolution of 12 bits. Polyamide particles (Griltex(R) 11A P82 from Ems-Chemie AG) with a size distribution of 80 – 200 µm are used as seeding particles. Additionally for each vortex 50 pictures are taken with a second camera (Nikon D90) mounted on a tripod, to measure the air core length of the vortices for all Froude numbers.

The experiments are conducted with a constant submergence of h = 110 mm and a constant temperature of T = 20 °C. Four different Froude numbers, Fr = 0.5, 0.7, 1.0 and 1.4, are investigated, see Table 1. For each Froude number the velocity fields are measured at three heights above the outlet, h_1 = 110 mm (surface), h_2 = 100 mm and h_3 = 10 mm. To guarantee the reproducibility, the flow is stopped between each measurement, until the water inside the vessel is completely stagnant. Then the flow is started again with the desired volume flow rate.

After the air core vortex has fully developed it is observed for 5 min before the start of the measurements, to make sure the vortex is stable. For each Froude number and height 4000 pictures are taken, which accords to a measurement time of the tangential velocity fields of 4 s each.

The PIV images are processed using the program PIVView2C from PivTec GmbH. Since the particle movement on two consecutive pictures is small, only every third picture is used for the evaluation. The velocity vectors are calculated using an adaptive cross-correlation method with a three step grid refinement. The grid sizes are 128 x 128 px, 96 x 96 px and 64 x 64 px, with an overlap of 50 %.

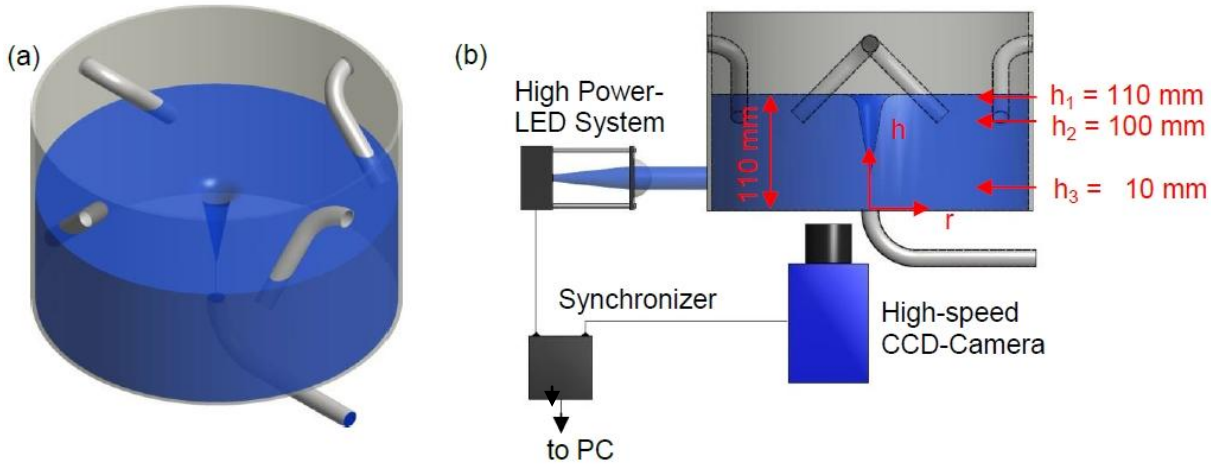

Figure 3: Inlet geometry shape and positioning in the vessel (a) and setup of High Power-LED System, including High-speed CCD-Camera and heights of measurement levels (b).

The pictures of the air core length are evaluated using a Matlab® script developed at the Institute of Multiphase Flows. The script measures the distance of the water surface to the outlet and the distance from the air core tip to the outlet for each picture. With a given submergence in meters the script calculates the mean air core length and the standard derivation for each vortex.

Table 1: Volume flow rates and corresponding Froude numbers for T = 20 °C and p = 1 atm

Volume flow rate Q/ $m^3 \cdot h^{-1}$	0.12	0.17	0.25	0.33
Froude number Fr/-	0.5	0.7	1.0	1.4

Results and discussion

Fig. 4a and 4b each show the time average velocity field for Fr = 1.4 at different heights. Since the experimental setup leads to a symmetrical vortex, the effect of vortex wandering doesn't occur and can therefore be neglected in the calculation of the time average.
For the tangential velocities the position of the vortex center was determined on each height level. From this position a vertical slice in y-direction with a width of one grid was chosen. Along the point of the grid all magnitudes of the velocity vectors were calculated and shifted so that the position of the outlet is the same on all height levels. The resulting velocities are shown for each Froude number and height in Fig. 5 – 7. As shown by Keller et al. the radial velocity is very low compared to the tangential velocity, especially close to the vortex center, see Keller et al. 2014. Therefore the shown velocities are essentially the tangential velocities of the vortex flow. It is visible from Figure 5 – 7 that different Froude numbers result in different tangential velocities. With an increase in the Froude number the tangential velocity also increases. On the surface the tangential velocities for the Froude numbers 0.7 – 1.4 show a maximum at distances of 8, 9 and 11 mm from the vortex center.

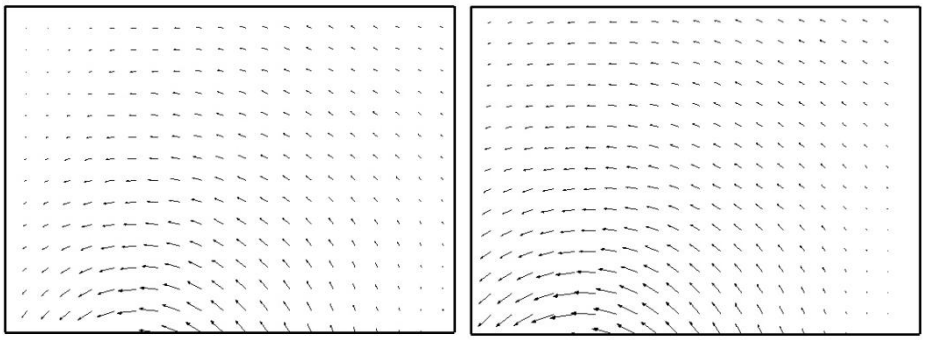

Figure 4: Velocity vector fields for: (a) Fr = 1.4, h_1 = 110 mm & (b) Fr = 1.4, h_1 = 100 mm.

The tangential velocities are different for each height regardless of the Froude number, see Fig. 8. While the tangential velocities for the Froude numbers 0.5 and 0.7 are still similar at all heights, for the Froude numbers 1.0 and 1.4 the tangential velocity increases with the depth. This is in accordance to the CFD simulations made by Pandazis et al., which show an increase in the tangential velocity near the outlet region, see Fig. 9. Also visible in Fig. 8 is the shift in the maximum of the tangential velocity for the Froude number 1.4 from the surface level (h_1 = 110 mm) to the level of h_2 = 100 mm. This is also shown in the CFD simulations of Pandazis et al. (Fig. 9) where the vortex core radius and therefore the maximum of the tangential velocity decreases with the depth, see also Pandazis et al. 2013. A possible influence of the air core radius on the radius of the vortex core near the surface, as well as the influence of surface effects, needs to be investigated.
In Fig. 10 the tangential velocity for Fr = 1.4 and h_1 = 110 mm is plotted in a diagram together with the tangential velocities calculated with the Rankine and the Burgers-Rott vortex model. The models are calculated using the maximum velocity and the vortex core radius gained from the experimental values. To fit the curve of the Burgers-Rott model to the curve of the experimental values the suction parameter a is chosen to be 0.039 $mm^2 \cdot s^{-1}$. It can be seen in the diagram that the maximum of the Rankine vortex model and thus the border of the vortex core can be fitted to the experimental values. The maximum of the Burgers-Rott model can be fitted to have the same maximum velocity value, but the maximum is closer to the vortex center, resulting in a smaller vortex core radius. The vortex core radius of the Burgers-Rott model matches the radius of the outlet. Outside the vortex core region both vortex models display the same values, with a 20 – 25 % deviation below the experimental results, which vanishes with increasing radius.

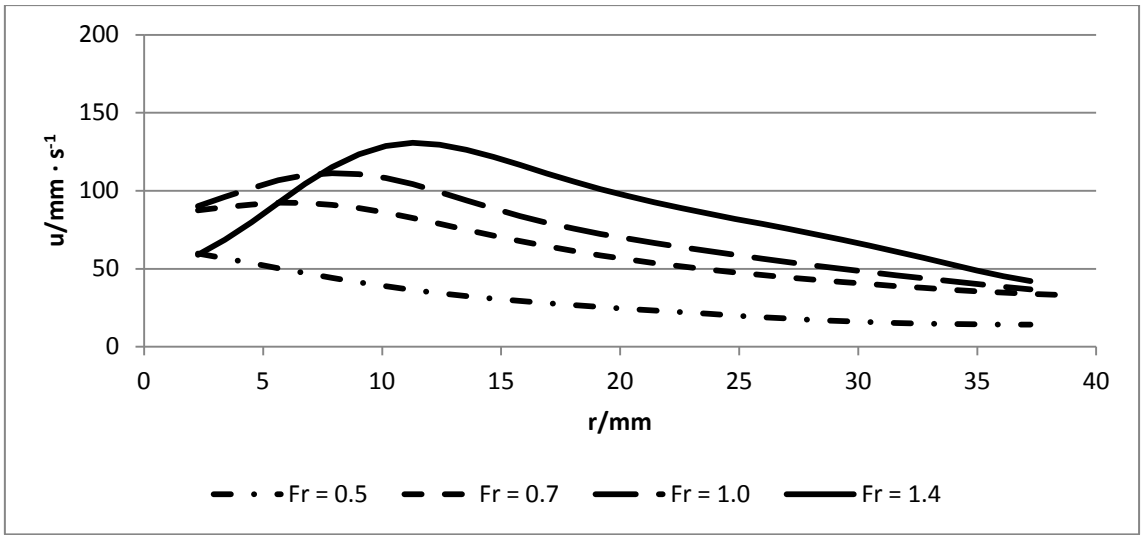

Figure 5: Velocity magnitude on the surface level h_1 = 110 mm.

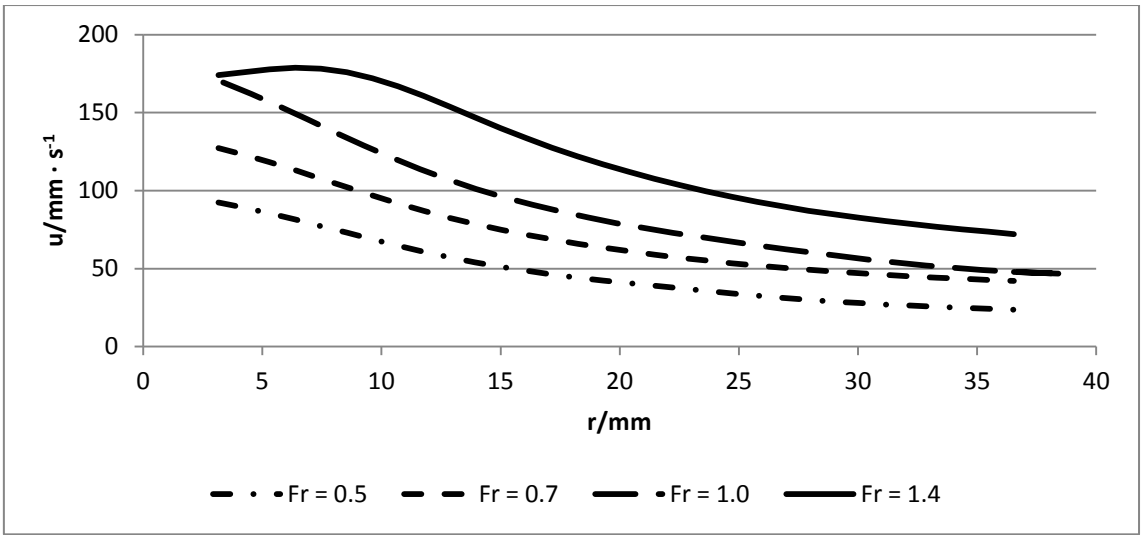

Figure 6: Velocity magnitude at h_2 = 100 mm above the outlet.

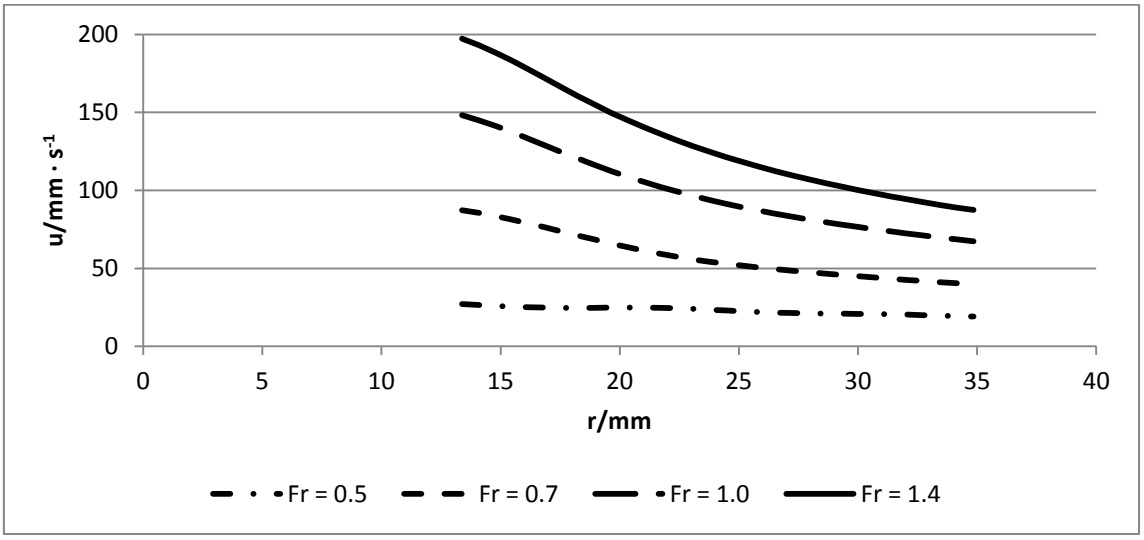

Figure 7: Velocity magnitude at h_3 = 10 mm above the outlet.

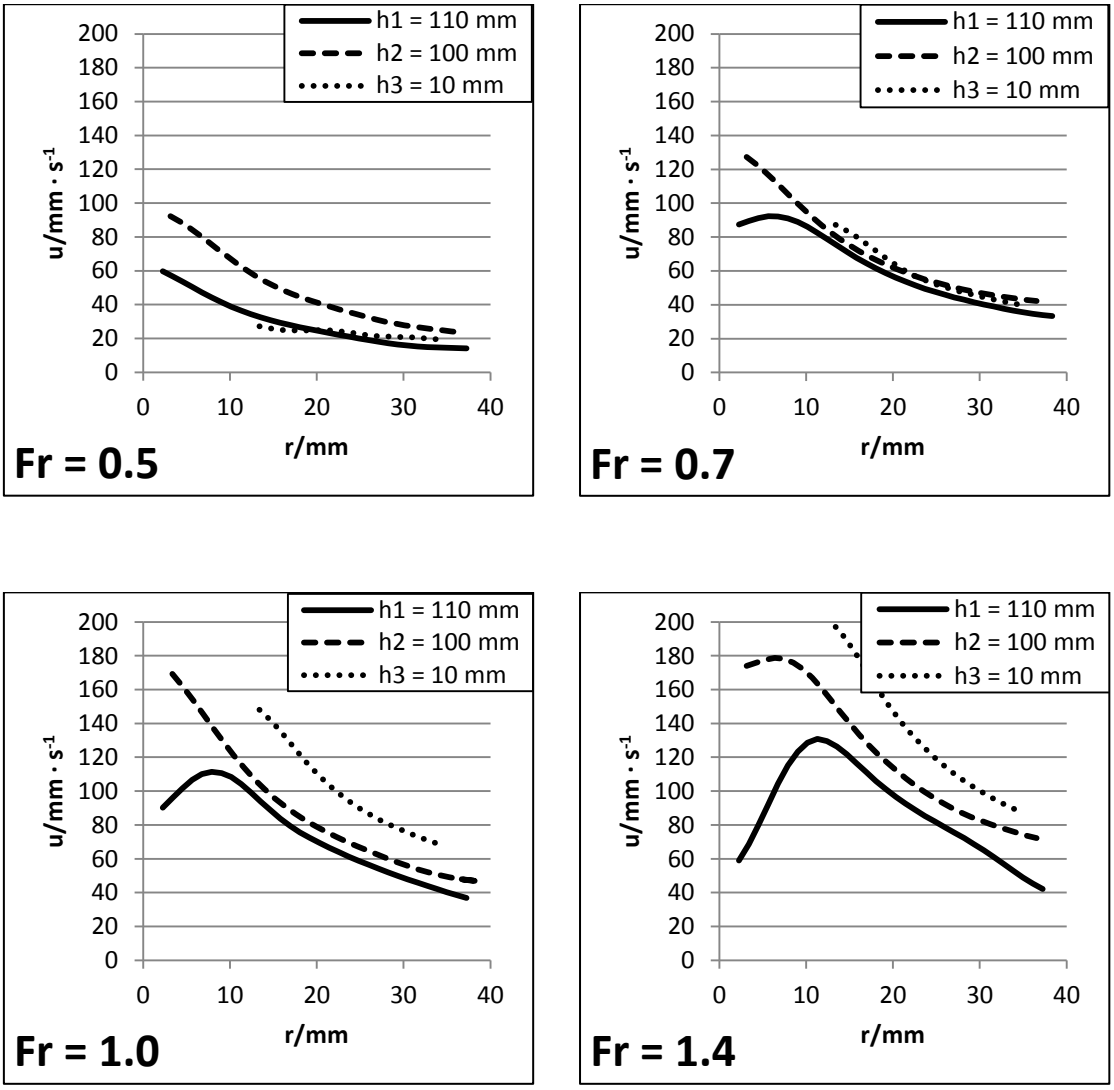

Figure 8: Velocity magnitudes for three heights and the Froude numbers 0.5 - 1.4.

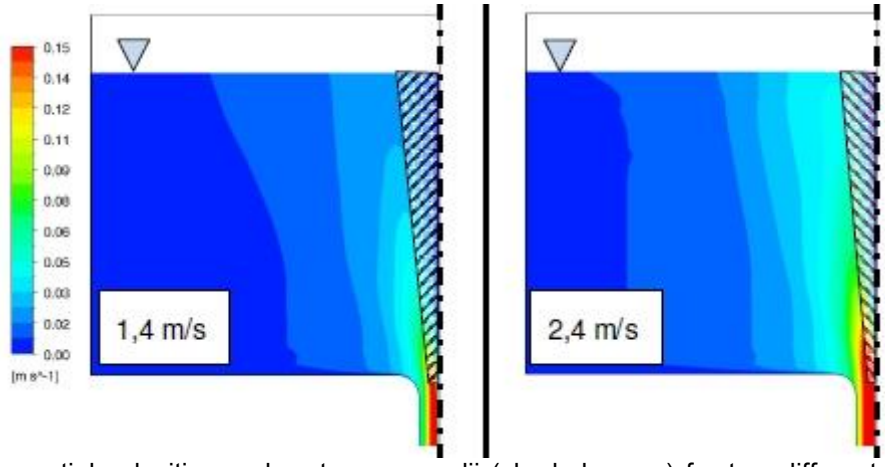

Figure 9: Tangential velocities and vortex core radii (shaded areas) for two different inlet velocities gained by CFD simulations, Pandazis et al. 2013.

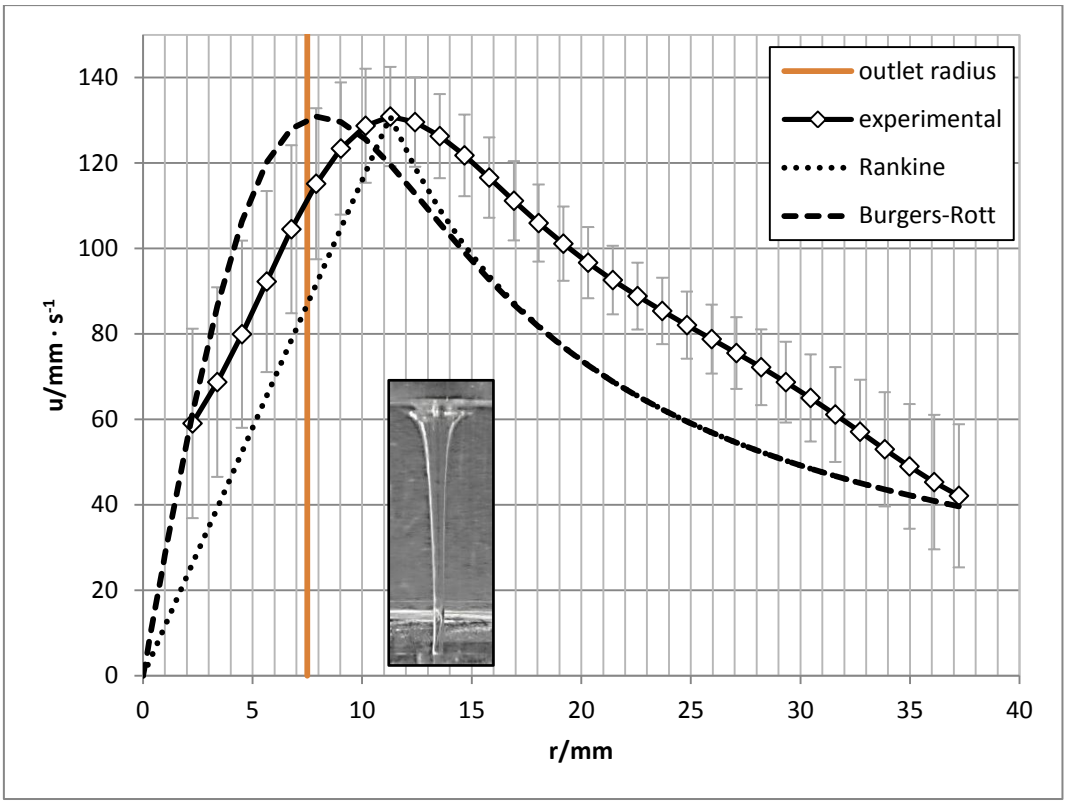

Figure 10: Tangential velocity profiles for experimental results and calculated with the Rankine- and the Burger-Rott vortex models for Fr = 1.4 and h_1 = 110 mm, plotted over the radius. Also included is the radius of the outlet and a picture of the air core vortex.

Conclusions & Outlook

The PIV system with a High-Power LED proves to produce good results. Furthermore the handling of the LED system is faster and less dangerous than the usage of a laser as a light source. Another advantage is that due to the lower energy output no problems with reflections of the air core or the water surface occurred, while it is still possible to conduct high-speed PIV measurements. The High-Power LED system can particularly be implemented in experiments where a steady 2D-flow is dominant.

The advantage of a high-speed PIV measurement is the possibility to variate the step size of the picture sequence for the evaluation even after the measurements. The step size can be chosen in dependence of the particle movement between two pictures, as shown in the method section of this paper. A next step is to implement a multistep evaluation which allows the setting of a region of interest on the pictures, which has a smaller step size then the rest of the picture. This would enable even more detailed results for flows with high velocity gradients, like vortices, where the particle movement increases towards the core region.

For the validation of the experiments it is necessary to evaluate the measured air core length and compare them with air core length calculated with the Burgers-Rott model. Further experiments will be conducted with a variation of the inflow angle to determine the influence of the angular momentum on the air core vortex. For the validation of the theoretical model the axial velocities at the border of the vortex core as well as the radial velocities at different heights need to be measured.

Additionally all experiments will also be conducted in a pilot plant with an upscale factor of 13.3, which corresponds to an inlet diameter of 0.2 m, a vessel diameter of 4.0 m and a submergence of 1.43 m.

Acknowledgements

This project is funded by the German Federal Ministry of Education and Research. Project number: 02NUK023A.

Symbols

a	suction parameter	g	gravitational constant
d	diameter	Fr	Froude number
h	submergence/height	Q	volume flow
h_∞	height outside the vortex core	T	temperature
L	air core length	p	pressure
r	radius	Γ	circulation
r_m	vortex core radius	Γ_∞	circulation outside the vortex core
u	velocity	v	kinematic viscosity
u_t	tangential velocity	λ	wave length
u_r	radial velocity		
u_z	axial velocity		

Literature

Batterson, J.W., et al., 2007: “Advancements in Theoretical Models of Confined Vortex Flowvields, University of Tennessee Space Institute, Tullahoma

Burgers J., 1948: “A mathematical model illustrating the theory of turbulence”, Adv Appl Mech No.1, pp.171–199

Chen, Y. et al., 2007; “Hydraulic Characteristics of Vertical Vortex at Hydraulic Intakes”, J. of Hydrodynamics, Ser. B, vol. 19(2), pp. 143 – 149

Hecker, G., 1987: “Fundamentals of vortex intake flow”, in: “Swirling flow problems at intakes”, Knauss J, (editor) IAHR hydraulic structures design manual No 1. Balkema, Rotterdam, NL, pp. 13– 38

Ito, K. et al., 2010: “Improvement of Gas Entrainment Prediction Method, Introduction of Surface Tension Effect”, J. of Nuclear Science and Tech., vol 47, No. 9

Keller, J. et al., 2014: “PIV measurements of air-core intake vortices”, Flow Measurement and Instrumentation, vol. 40, pp. 74 – 81

Knauss, J., 1983: „Wirbelbildung an Einlaufbauwerken- Luft- und Dralleintrag“, Verlag Paul Parey, Hamburg und Berlin

Odgaard, A.J., 1986: ”Free-Surface Air Core Vortex”, J. of Hydraulic Engineering, vol. 112, no. 7, pp. 610 – 620

Pandazis, P. et al., 2010: „Potential von ANSYS CFX 12 zur Bestimmung der erforderlichen Mindestüberdeckung von Ansaugstutzen von Pumpen zur Vermeidung von Luftmitriss“, Fachbericht zur Jahrestagung Kerntechnik 2010,TÜV NORD SysTec GmbH & Co. KG

Pandazis, P. et al., 2013: „Generic numerical determination of the critical submergence at pump intakes to avoid gas entrainment, Fachbericht zum BMBF Förderprojekt Nr. 1501410, TÜV NORD SysTec GmbH & Co. KG

Rott, N., 1958: “On the Viscous Core of a Line Vortex”, Zeitschrift für angewandte Mathematik und Physik ZAMP, vol. 9, Issue 5-6, pp. 543 – 553

Suerich-Gulick, F. et al., 2014: “Free surface intake vortices: theoretical model and measurements”, Journal of Hydraulic Research, vol. 52, no. 4, pp. 502-512